The American Journal of Pathology, Vol. 175, No. 6, December 2009

DOI: 10.2353/ajpath.2009.090185

Vascular Biology, Atherosclerosis and Endothelium Biology

Septoclast Deficiency Accompanies Postnatal Growth Plate Chondrodysplasia in the Toothless (*tl*) Osteopetrotic, Colony-Stimulating Factor-1 (CSF-1)-Deficient Rat and Is Partially Responsive to CSF-1 Injections

Alison Gartland,* April Mason-Savas,*† Meiheng Yang,* Carole A. MacKay,* Mark J. Birnbaum,‡ and Paul R. Odgren*

From the Departments of Cell Biology and Orthopedics,† University of Massachusetts Medical School, Worcester, Massachusetts; and the Department of Biology,‡ Merrimack College, North Andover, Massachusetts*

The septoclast is a specialized, cathepsin B-rich, perivascular cell type that accompanies invading capillaries on the metaphyseal side of the growth plate during endochondral bone growth. The putative role of septoclasts is to break down the terminal transverse septum of growth plate cartilage and permit capillaries to bud into the lower hypertrophic zone. This process fails in osteoclast-deficient, osteopetrotic animal models, resulting in a progressive growth plate dysplasia. The *toothless* rat is severely osteopetrotic because of a frameshift mutation in the colony-stimulating factor-1 (CSF-1) gene (*Csf1*^{tl}). Whereas CSF-1 injections quickly restore endosteal osteoclast populations, they do not improve the chondrodysplasia. We therefore investigated septoclast populations in *Csf1*^{tl}/*Csf1*^{tl} rats and wild-type littermates, with and without CSF-1 treatment, at 2 weeks, before the dysplasia is pronounced, and at 4 weeks, by which time it is severe. Tibial sections were immunolabeled for cathepsin B and septoclasts were counted. *Csf1*^{tl}/*Csf1*^{tl} mutants had significant reductions in septoclasts at both times, although they were more pronounced at 4 weeks. CSF-1 injections increased counts in wild-type and mutant animals at both times, restoring mutants to normal levels at 2 weeks. In all of the mutants, septoclasts seemed misoriented and had abnormal ultrastructure. We conclude that CSF-1 promotes angiogenesis at the chondroosseous junction, but that, in *Csf1*^{tl}/*Csf1*^{tl} rats, septoclasts are unable to direct their degradative activity appropriately, implying a capillary guidance role for locally supplied CSF-1. ***(Am J Pathol 2009, 175:2668–2675; DOI: 10.2353/ajpath.2009.090185)***

The majority of skeletal elements, including limb bones, the vertebral column, ribs, pelvis, digits, and the posterior mandible, grow via the process of endochondral ossification in which a cartilage anlage, or model, is first formed and subsequently replaced by bone.[1,2] This is necessitated by the fact that bone, which is rigid, cannot expand interstitially, but can only grow at its surface by bone deposition. To protect the growing cartilage from the rigors of excessive mechanical loading, a secondary ossification center develops to support the articular cartilage of the joint, and the growth cartilage forms into a growth plate across the end of the bone shaft, separating the epiphysis from the metaphysis.[3,4] Chondrocytes in the growth plate proliferate, undergo expansion, or hypertrophy, and drive bone elongation. This process has been well studied and is regulated by complex interactions among many growth factors and morphogens, including Indian Hedgehog, parathyroid hormone-related protein, insulin-like growth factors, and other regulatory

Supported by National Institute for Dental and Craniofacial Research, National Institutes of Health (grants DE13961 and DE07444 to P.R.O.).

Opinions expressed are the responsibility of the authors and do not necessarily reflect those of the National Institute for Dental and Craniofacial Research or the National Institutes of Health.

Accepted for publication August 6, 2009.

Current address of A.G.: Mellanby Centre for Bone Research, The University of Sheffield, Sheffield, United Kingdom, and C.A.M.: Center for Restorative and Regenerative Medicine, Providence Veteran's Administration Hospital, Providence, Rhode Island.

Address reprint requests to Paul R. Odgren, Ph.D., Department of Cell Biology, University of Massachusetts Medical School, 55 Lake Ave. N., Worcester, MA 01655. E-mail: paul.odgren@umassmed.edu.

pathway components (reviewed in 5,6). The growth cartilage is ultimately resorbed and replaced by bone. This conversion from cartilage to bone takes place along the chondroosseous junction (COJ), and it requires that cartilage, which is avascular, be invaded by blood vessels that carry with them bone-resorbing and bone-forming cells.

Chondrocytes of the growth plate are normally highly organized spatially with respect to cell differentiation. The uppermost cell population is called the resting zone. Its cells are nonproliferative and serve as a reserve pool for future growth. The cells of the proliferating zone are immediately subjacent, typically occupy roughly the upper half of the growth plate, and are active in the cell cycle and at the same time are secreting significant amounts of cartilage matrix. After several days, the cells cease proliferating, switch from expression of type II to type X collagen, and begin to swell, or become hypertrophic, expanding up to 10 times in height within 1 to 2 days.[7–9] They also secrete matrix vesicles, which mineralize the matrix. Ultimately, capillaries invade from the metaphyseal side, and osteoclasts (also called "chondroclasts" at this location) attach to and consume roughly two of three of the longitudinal cartilage septa, the vertical walls that divide the chondrocyte columns. The remaining longitudinal septa comprise the substrate onto which osteoblasts deposit the bone of the primary spongiosa. During rapid growth, this area is the site of intense metabolic activity, with bone resorption and formation taking place within a few micrometers of each other. Added to these complex metabolic processes are the growth of vasculature and establishment of hematopoietic marrow.

The septoclast is a specialized, perivascular cell that facilitates capillary invasion of the chondroosseous junction.[10] Septoclasts are rich in the protease cathepsin B, and they are located such that the cell body and nucleus lie just behind the budding end of the capillary. Their cytoplasm extends toward the growth plate and takes on a ruffled border-like appearance adjacent to the terminal transverse septum of the growth plate. It has been inferred that this cell type is required for the continued growth of blood vessels into the growth plate, thus permitting normal bone elongation to occur.[10]

In some animal models of osteopetrosis, a condition in which defective bone resorption by osteoclasts leads to a sclerotic skeleton, we and others have noted an accompanying pathological change in the growth plate. The *toothless* (*Csf1^{tl}*/*Csf1^{tl}*) osteopetrotic rat has a recessive, loss-of-function frameshift mutation in the gene for colony-stimulating factor-1 (CSF-1 or macrophage-CSF).[11,12] The loss renders the *Csf1^{tl}*/*Csf1^{tl}* rat severely osteopetrotic because of profound osteoclastopenia. In this strain, as in a growing list of osteoclast-deficient mutant mice,[13] there is a progressive dysplasia in which chondrocytes fail to form their normal columns and differentiation zones, the central region of the growth plate thickens with time, and vascular invasion at the COJ is deficient.[14–17] Injections of CSF-1 restore osteoclast populations and activity in the *Csf1^{tl}*/*Csf1^{tl}* rat and rescue some, but not all, aspects of the mutant phenotype.[15,18] Notably, the growth plate dysplasia remains unimproved despite daily CSF-1 injections beginning at birth, before the dysplasia develops, and continuing for 6 weeks.[15] The lower margin of the growth plate, rather than being a site for vessel budding and bone and cartilage remodeling, becomes covered with a layer of bone and the vessels are blunted and enlarged and do not penetrate the cartilage. Despite this lack of effect on the chondrodysplasia, it was shown that CSF-1 injections have a stimulatory effect on angiogenesis in the metaphysis of *Csf1^{tl}*/*Csf1^{tl}* rats as measured by vascular casts and electron microscopy,[14] at least in the short term.

CSF-1 is known to promote angiogenesis, primarily through the stimulation of VEGF secretion.[19] Depletion of VEGF has been shown to block vascularization of the growth plate.[20] Because of the association between septoclasts and vascular invasion of the growth plate, we wished to investigate septoclast populations in *Csf1^{tl}*/*Csf1^{tl}* rats and their possible response to CSF-1 treatment. We also wished to further investigate the septoclasts themselves in normal animals and to document their relation to other cell types at the COJ, because relatively little is presently known about them. We report here the results of histological, immunohistochemical, and electron microscopic investigations of this specialized perivascular cell population in wild-type and *Csf1^{tl}*/*Csf1^{tl}* mutant rats with and without CSF-1 treatments.

Materials and Methods

Animals and Treatments

Mutant (*Csf1^{tl}*/*Csf1^{tl}*) and wild-type (+/+) rats of the *toothless* strain were obtained from breeding colonies maintained under pathogen-free conditions at the University of Massachusetts Medical School. All procedures involving animals were performed under protocols approved by the Institutional Animal Care and Use Committee. Two ages were studied: 2 and 4 weeks. Some animals were treated beginning 1 week before sacrifice with injections of recombinant human CSF-1 (kindly provided by Chiron, Emeryville, CA). Rats received a daily s.c. injection of 10^6 units in sterile saline, a dose that results in roughly normal circulating levels of CSF-1 and which restores high numbers of osteoclasts in the tibial metaphysis within 4 days.[21] Control animals received just saline. All experimental groups contained at least three individual animals. Mice for CD-34 labeling were 2-week-old wild-type animals from our *op*/*op* mouse colony.

Tissues and Labeling

Animals were sacrificed at the appropriate times and tibiae were dissected, promptly split longitudinally, and fixed by immersion in ice-cold fixative. For electron microscopy and high-resolution histological analysis, samples were fixed overnight at 4°C in 0.1 mol/L cacodylate buffer containing 2.5% glutaraldehyde (Polysciences,

Warrington, PA) or in the same fixative supplemented with 0.7% ruthenium hexaamine trichloride (Polysciences) to preserve chondrocyte morphology.[22] They were then rinsed in cacodylate buffer and demineralized by incubation in the cold in 12.5% disodium EDTA, pH 8.0, for up to 2 weeks, as needed. Tissues were postfixed for 1 hour in 1% osmium tetroxide, dehydrated in a graded series of ethanol solutions followed by propylene oxide, and infiltrated overnight in Epon (JB-4, Polysciences) mixed 2:1 v/v with propylene oxide in BEEM capsules. They were baked for 48 hours. For light microscopic images of Epon-embedded samples, 2-μm sections were cut and stained with 0.1% toluidine blue. For transmission electron microscopy, 90-nm sections were cut and stained with uranyl acetate/lead citrate.

For immunohistochemical analysis, bones were fixed in 4% paraformaldehyde overnight at 4°C, rinsed in PBS, and then demineralized as above. They were dehydrated with ethanol followed by xylene and paraffin embedded, and 5-μm sections were cut. For comparisons of endothelial cells (von Willebrand factor for rats, CD-34 for mice) versus septoclasts (cathepsin B) and for c-Fms localization, 3-μm serial sections were cut. Sections were deparaffinized in xylene and rehydrated, and an antigen retrieval procedure was performed as follows. Slides were placed in Coplin jars filled with 0.01 mol/L citric acid buffer, pH 6.0. The jars were placed in a microwave oven and subjected to pulse-heating as follows. They were brought to a boil and the power was turned off. After 1 minute power was turned on to return to a boil and then switched off, and this cycle was repeated 10 times, after which the jars were placed at ambient temperature for 20 minutes followed by a brief rinse in room temperature water. Endogenous peroxide was blocked by a 10-minute incubation in 3% H_2O_2, and nonspecific binding was blocked by a 20-minute incubation in 5% normal goat serum diluted in PBS. After blocking, primary antibodies, diluted in 1% normal goat serum in PBS, were applied and incubated overnight at 4°C. Primary antibodies were rabbit anti-rat cathepsin B and anti-rat cathepsin K (kindly provided by Dr. John S. Mort[10]), rabbit anti-tartrate-resistant acid phosphatase (kindly provided by Dr. Göran Andersson), rabbit anti-von Willebrand factor, rabbit anti-mouse CD-34, and rabbit anti-c-Fms (Abcam, Cambridge, MA). After three washes in PBS, secondary antibody, biotin-conjugated goat anti-rabbit IgG (Dako, Carpenteria, CA), was applied and incubated for 1 hour at room temperature. After three washes in PBS, avidin-biotin-horseradish peroxidase complex (Dako) was applied according to the manufacturer's instructions, the slides were washed with PBS, and diaminobenzidine substrate (Dako) was incubated on the sections to develop signal. Some sections were counterstained with hematoxylin, and some were counterstained with 0.1% toluidine blue.

Cell Counts

Septoclasts were counted in cathepsin B-stained sections along a line projected into the microscope field of view at the chondroosseous junction using descriptors developed from the original identification of the septoclast.[10] Because cathepsin B is ubiquitously expressed, distinguishing this cell population required combining several criteria. i) Immunochemical properties: only cells strongly labeled for cathepsin B in comparison with their nearest neighbors were counted. ii) Positional information: cells had to lie within one or two cell lengths of the bottom of the lower margin of the growth plate. If they were also adjacent to a terminal capillary bud in the section, this was taken as additional evidence. iii) Morphology: septoclasts typically have a characteristic, elongated morphology with a cell body and a single nucleus lying just behind and adjacent to the leading edge of the capillary and extend a cytoplasmic process toward the lower margin of the growth plate. If these properties were evident, they were taken as supporting evidence that a given cell should be counted. With these guidelines, septoclasts were counted using an Olympus BH2 microscope with a digitizing tablet attached that permitted the projection of a line of fixed length into the field of view, 775 μm long under a $\times$20 objective. The lateral margins, approximately 150 μm, of the COJ were not counted because they contain periosteum and perichondrium and also have some cathepsin B-rich cells that are not septoclasts (not vesicle-associated, rounder shape, not part of the COJ). In *Csf1^{tl}*/*Csf1^{tl}* mutants, especially at 4 weeks old, the entire central region of the growth plate often contained no cathepsin B-positive cells. Care was taken to position the counting line such that it represented both septoclast-containing and septoclast-free areas in roughly their correct proportions. Using these criteria, septoclasts were counted blind by three different individuals. At least three sections were counted per animal, and at least three individual animals were analyzed for each experimental group. Counts from the different experimental groups obtained by different individuals, from different sections, and from different individual animals were analyzed for consistency by *t*-tests for differences in sample means. When no statistically significant differences (95% confidence limits) were found to be due to these potential "nuisance variables," results were pooled for overall statistical analysis using 95% confidence limits (Microsoft Excel, Microsoft, Redmond, WA).

Results

Histological Evaluations of Normal and Mutant COJ

Epon sections permitted visualization of septoclasts at the COJ in normal rats, as described previously.[10] In Figure 1, we show a typical septoclast adjacent to a capillary bud invading the metaphyseal side of the proximal tibial growth plate in a 4-week-old normal rat. In Figure 1A, the toluidine blue staining shows a large, multinucleated osteoclast attached to two adjacent longitudinal septa. Above this is a capillary bud containing several blood cells. Adjacent to the capillary is a septoclast, with its cytoplasm extending up beyond the capil-

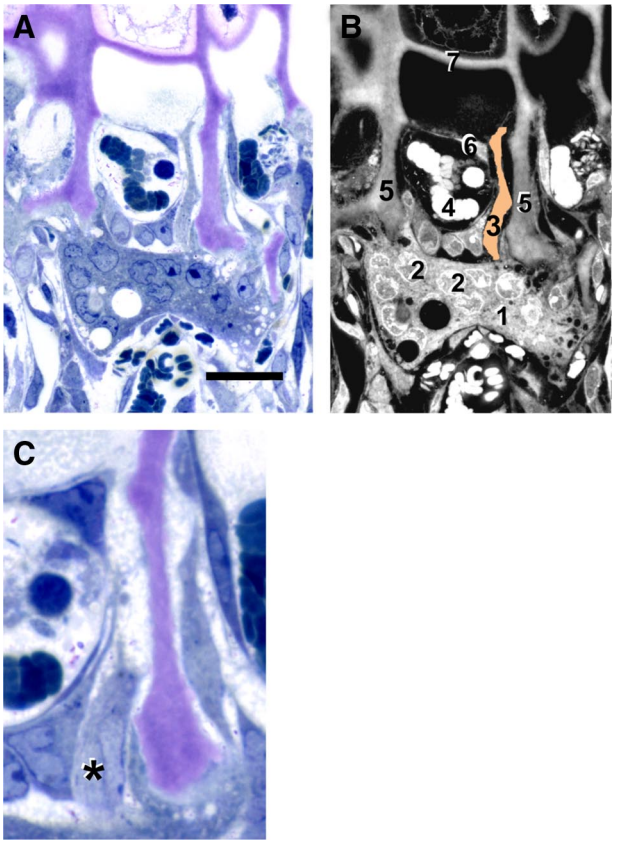

Figure 1. Septoclast in the context of the chondroosseous junction. **A:** Light micrograph of a 4-week-old wild-type rat proximal tibia stained with toluidine blue. **B:** diagram of **A** with various cellular and structural constituents numbered: 1, osteoclast; 2, some of the multiple nuclei in the osteoclast; 3, septoclast cell body and cytoplasmic extension, pseudo-colored light orange; 4, red blood cells in budding capillary; 5, longitudinal septa of the hypertrophic cartilage zone (cartilage matrix is stained purple due to toluidine blue metachromasia); 6, endothelial cell of the capillary; and 7, terminal growth plate transverse septum. A hypertrophic chondrocyte can be seen just above the transverse septum. **C:** Serial section to **A** at higher magnification in which the septoclast cell body and nucleus are visible, but the cytoplasmic extension is out of the plane. **Asterisk** is adjacent to the nucleus. Scale bars: 25 μm (**A**); 13 μm (**C**). Epon sections.

lary. A labeled diagram of the image is shown in Figure 1B. Figure 1C shows a serial section to Figure 1A, at a slightly higher magnification, that contains a profile of the septoclast cell body and nucleus. Similar sections of *Csf1*^{tl}/*Csf1*^{tl} rats consistently show a dysplasia of the growth plate and COJ (Figure 2, A–D), as described previously.[15,17,23] Capillaries become enlarged and fail to penetrate the hypertrophic lacunae at the lower margin of the growth plate.

Distinguishing Septoclasts from Osteoclasts and Endothelial Cells

We performed immunohistochemical staining for septoclasts using anti-cathepsin B[10] and for osteoclasts using anti-cathepsin K (Figure 3). Cathepsin K antibody clearly labeled osteoclasts (Figure 3, B and D), the other major catabolic cell type in this area of the tissue, and showed that they typically are localized behind the capillary front, below the chondroosseous junction. Virtually identical results were obtained with anti-tartrate-resistant acid phosphatase antibody (not shown). Cathepsin B antibody (Figure 3, A and C), on the other hand, intensely labeled a distinct cell population that is nearer to the growth plate than the osteoclasts, and whose morphology is strikingly different, typically showing very elongated forms directed

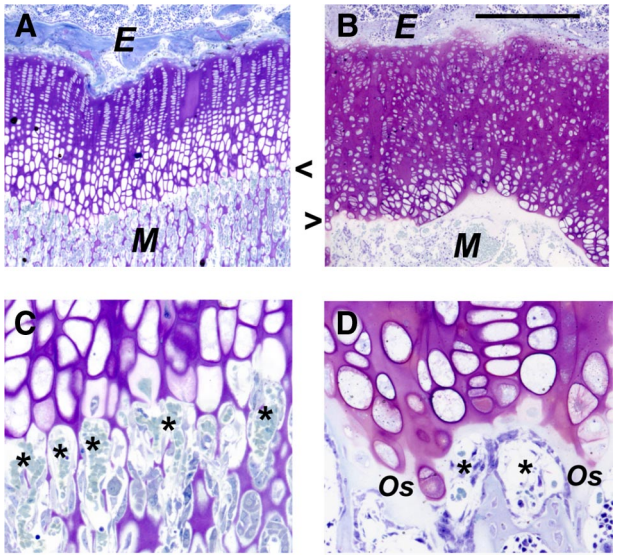

Figure 2. Growth plate dysplasia in the *Csf1*^{tl}/*Csf1*^{tl} rat. **A** and **C:** Four-week-old wild-type rat. **B** and **D:** Mutant littermate rat proximal tibia growth plates (Epon sections stained with toluidine blue). **B:** Thickening, irregularity, and loss of differentiation zones in this postnatal chondrodysplasia. **C** and **D:** Higher magnification of the chondroosseous junctions. Several capillaries invading the metaphyseal side are indicated (**asterisks**). In the mutant, vessels are blunted and do not enter the growth plate. A layer of osteoid (Os) bony matrix seals off the lower edge of the growth plate. **Arrowheads** indicate the COJ. E, epiphysis; M, metaphysis. Scale bars: 400 μm (**A** and **D**); 100 μm (**C** and **D**).

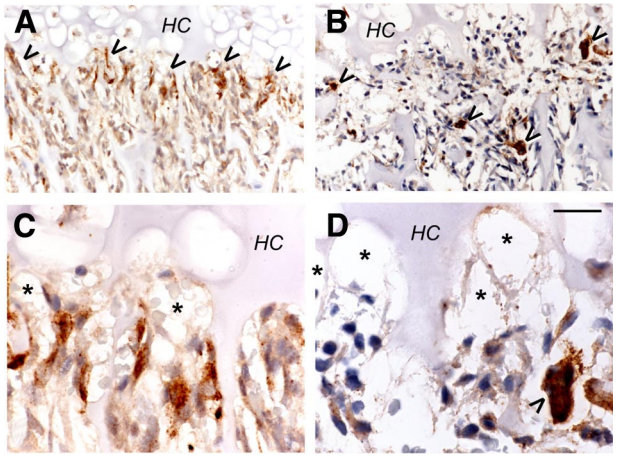

Figure 3. Cathepsin B and K immunostaining of the chondroosseous junction (2-week-old wild-type rat proximal tibia; 5-μm paraffin sections). Peroxidase immunostaining is brown, with hematoxylin counterstain. **A** and **C:** Cathepsin B. **B** and **D:** Cathepsin K. Septoclasts along the COJ are labeled by anti-cathepsin B antibody (**arrowheads** in **A**), and the osteoclasts, the other main catabolic cell type in this area, are intensely stained by anti-cathepsin K (**arrowheads** in **B**). HC, hypertrophic chondrocyte zone of the growth plate. Septoclasts lie along the COJ, whereas the osteoclasts are distal to the COJ. Higher magnification shows that the cathepsin B staining is confined to cells immediately adjacent to the capillaries (**asterisks** in **C** and **D**), whereas the osteoclast (**arrowhead**) is behind the capillary termini. Thus, the cathepsin B-labeled cells are not osteoclasts. Scale bar: 61.3 μm (**A** and **B**); 20 μm (**C** and **D**).

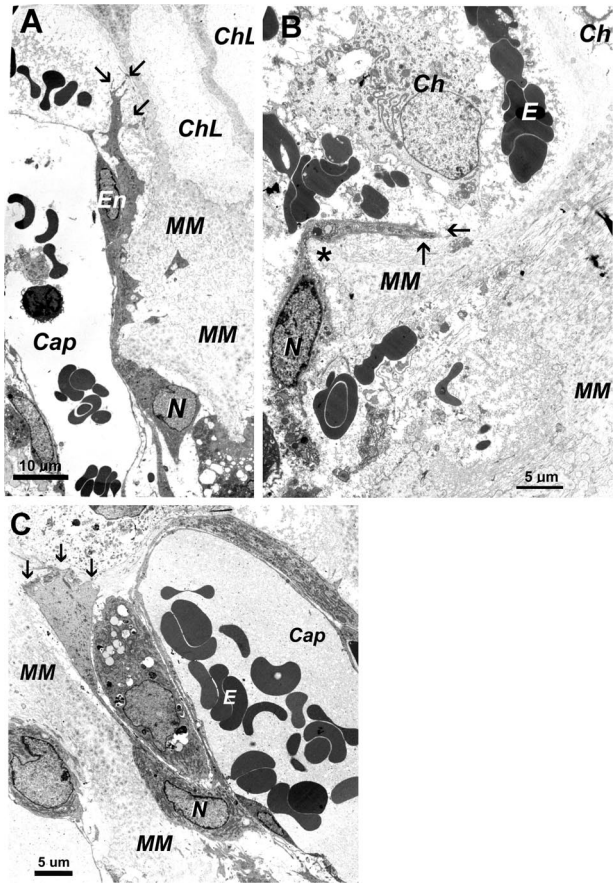

Figure 4. Electron micrographs of septoclasts in 2-week-old normal rats and *Csf1^{tl}/Csf1^{tl}* rats with and without CSF-1 treatment. Sections are from the proximal tibial COJ. **A:** A typical septoclast is seen in a normal rat extending along a capillary (Cap), containing blood cells, up toward the lower margin of the growth plate. The septoclast nucleus (**N**) is in the cell body and the cytoplasm is highly extended toward the growth plate and passes between mineralized matrix (MM) (although demineralized in these sections) and the endothelial cell lining the capillary. Two chondrocyte lacunae (ChL) are visible near the top. The upper end of the septoclast forms several small projections (**arrows**). **B:** The COJ of an untreated *toothless* rat is highly disorganized. Although rare, septoclasts like the one shown were found. The cell in **B** is misoriented. Its cytoplasmic extension makes a sharp turn (**asterisk**) adjacent to a mature chondrocyte (Ch) and ends in a single projection (**arrows**). **C:** CSF-1 treatment produced a larger population of more normal-looking septoclasts. In this panel, the cell located between the septoclast cell body and the capillary wall seems to be a pericyte. E, erythrocytes; En, endothelial cell body with nucleus.

toward the growth plate. Staining for cathepsin B and for the endothelial marker, Von Willebrand factor, consistently showed stained cells that lay above the septoclast cell bodies in serial sections. Similar results were obtained using serial sections of mouse proximal tibia COJ with anti-CD-34 (not shown). Together with the Epon histology (Figure 1), transmission electron microscope images (Figure 4, A–C), and the earlier work by Lee et al,[10] we concur that the septoclast is a distinct, catabolic cell type that accompanies vessels at the COJ.

Septoclasts at the Dysplastic COJ of Toothless Rats and Their Responses to CSF-1

We treated *Csf1^{tl}/Csf1^{tl}* rats for 1 week before sacrifice with recombinant human CSF-1 at a dose that restores osteoclast populations within 4 days and significant marrow spaces within 6 days.[21] Electron micrographs from these experiments are shown in Figure 4. Wild-type 2-week-old rats (Figure 4A) had typical septoclasts, with cell bodies and nuclei lying below the leading edge of the budding capillary and extending a long cytoplasmic processes between the endothelial cell and the mineralized cartilage matrix into which it was budding. The cell shown terminates in several cytoplasmic branches, which have been shown at higher magnification to form a ruffled edge along the last transverse septum of the growth plate.[10] In the *Csf1^{tl}/Csf1^{tl}* rats, septoclasts were difficult to identify because of the severely dysplastic COJ. Among those we could locate, the one shown in Figure 4B is representative: the septoclasts seem misdirected, with the cytoplasmic extension taking a right-angle turn, not clearly associated with endothelium and not forming a branching terminus. In contrast, when mutant animals were treated with CSF-1, septoclasts were easier to identify; they had taken on more typical appearances and were generally associated with vessels (Figure 4C).

Figure 5, A–H, presents anti-cathepsin B-labeled overviews of proximal tibial COJs of the different genotypes, ages, and treatment groups in this study. We saw consistently that mutant rats had strikingly fewer septoclasts than wild-type animals at both 2 and 4 weeks. In addition, when wild-type animals were treated with CSF-1, their septoclast populations seemed to increase. Likewise when *Csf1^{tl}/Csf1^{tl}* rats were treated with CSF-1, the overall cathepsin B labeling at the COJ also increased. The panels in Figure 5 are representative of the sections that were used for quantitative assessments by counting. Counts of septoclasts had not been performed before; therefore, a method was devised in which several criteria were combined, including intensity of cathepsin B staining, position, and cell morphology (see *Materials and Methods*). Multiple sections from tissue blocks from multiple animals were counted blindly by three different individuals. For the specific blocks from which the sections shown in Figure 5 were cut, the counts were (Figure 5A) 15.7 ± 4.8, (Figure 5B) 9.0 ± 4.8, (Figure 5C) 18.7 ± 8.5, (Figure 5D) 11.6 ± 3.1, (Figure 5E) 18.9 ± 3.6. (Figure 5F) 25.2 ± 3.8, and (Figure 5G) 10.8 ± 5.9 (mean ± SD, $n = 9$). To demonstrate further the nature of the counts that were performed, higher-magnification panels of regions of each of the panels are shown in Figure 6, A–H, with individual septoclasts indicated by arrows.

Septoclast counts and *t*-tests for significance of differences between groups are shown in Figure 7. *Csf1^{tl}/Csf1^{tl}* rats at both 2 and 4 weeks had significantly fewer septoclasts (8.48 and 5.85, respectively) than normal littermates (15.31 and 20.0, $P < 0.00001$ for both). CSF-1 treatment significantly increased the septoclast counts in wild-type animals at both 2 weeks (19.67, $P < 0.01$) and 4 weeks (26.59, $P < 0.00001$), and it also increased the counts in mutants at both ages (13.44 and 10.37, $P < 0.00001$ for both). Differences between treated wild-type and treated mutant animals were also highly significant at both ages ($P < 0.00001$). Treatment with CSF-1 restored septoclast counts in 2-week-old mutants to the level seen

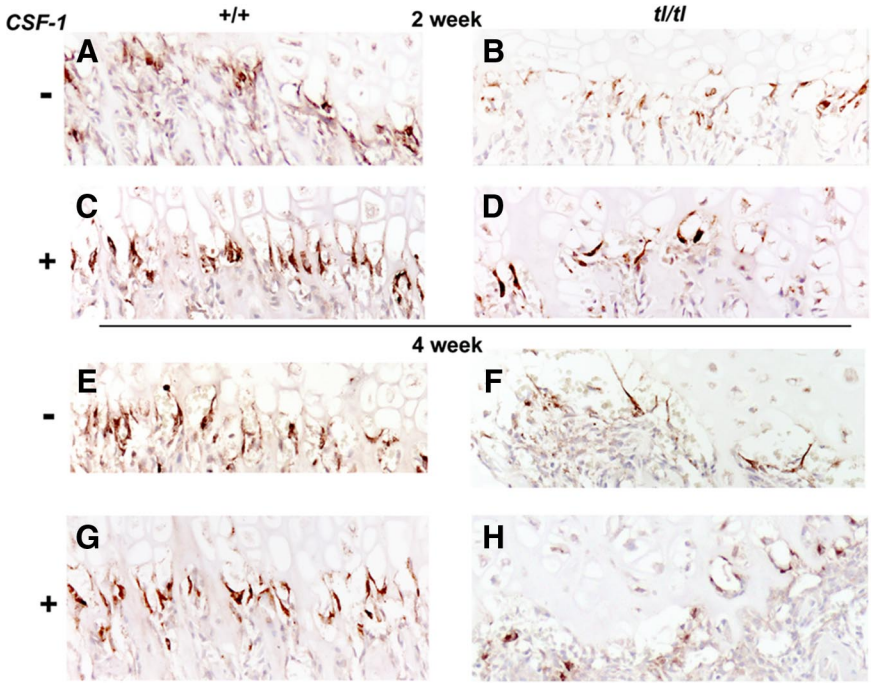

Figure 5. Septoclasts in wild-type (+/+) and *Csf1*^{tl}/*Csf1*^{tl}(*tl*/*tl*) rats with and without CSF-1 injections. Wild-type rat COJs (**A, C, E,** and **G**) have abundant septoclasts organized along the invading capillary front at the COJ, shown by cathepsin B immunolabeling (brown color), at 2 (**A** and **C**) and 4 (**E** and **G**) weeks postpartum, whether untreated (**A** and **E**) or injected with CSF-1 (**C** and **G**). In *tl* mutants (**B, D, F,** and **H**) there are fewer septoclasts, and their distribution is less organized. At 2 weeks (**B** and **D**), septoclast populations are closer to normal, and the staining intensity was greater than at 4 weeks (**F** and **H**). Cell counts were performed on these and similar sections (paraffin sections labeled with anti-cathepsin B and lightly counterstained with hematoxylin).

in untreated normal littermates ($P > 0.05$), but differences between all other groups were highly significant.

Finally, given the partial responses of septoclast populations to CSF-1 injections, especially at the 2-week age, we investigated whether the effect of CSF-1 could be in part due to a direct stimulation of septoclasts themselves. Labeling for c-Fms, the CSF-1 receptor, and for cathepsin B was done on adjacent sections from the experimental groups, and the results for a normal, 2-week-old rat are shown in Figure 8. Very strongly labeled, cathepsin B-positive septoclasts are seen at the COJ (Figure 8A), whereas no strong label is seen with anti-c-Fms (Figure 8B). An osteoclast from a field nearby to that shown in Figure 8B is shown in Figure 8C, and it is strongly positive for c-Fms, serving as a positive control for the specificity of the label, which indicates that the effects of CSF-1 on septoclasts are indirect. Septoclasts were not labeled in any of the experimental groups (others not shown).

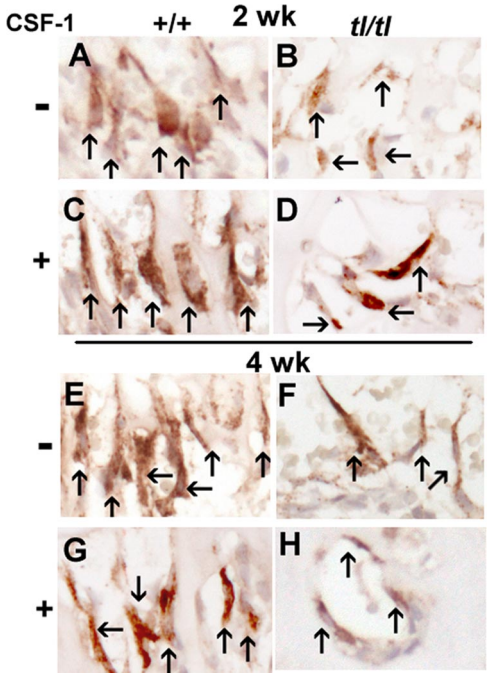

Figure 6. Counting septoclasts in cathepsin B-labeled sections. The panels show enlargements of regions of sections shown in Figure 5 with individual septoclasts indicated by **arrows**. The criteria for counting were based on position, morphology, and intensity of labeling, as described.

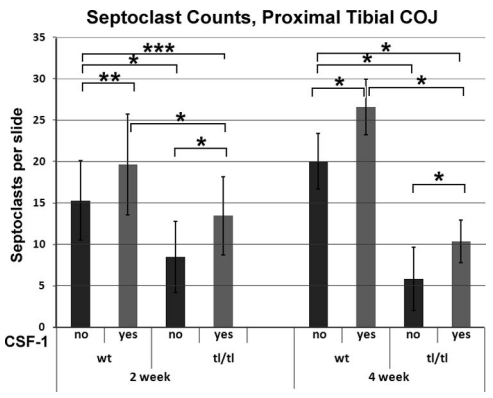

Figure 7. Septoclast counts in *Csf1*^{tl}/*Csf1*^{tl} rats (*tl*/*tl*) and their wild-type littermates (wt). Animals were untreated or treated with daily injections of CSF-1 for 1 week before sacrifice. Mean count per slide plus 1 SD is shown. The septoclast counts in mutant animals were lower than those in normal littermates at 2 weeks and fell much further behind by 4 weeks. CSF-1 increased the septoclast counts in both genotypes at both ages, bringing counts to normal levels in mutants at 2 weeks, but having a much more modest effect at 4 weeks. For wild-type untreated, $n = 29$ at 2 weeks, $n = 27$ at 4 weeks; for wild-type treated with CSF-1, $n = 27$ for both time points; for *tl*/*tl* untreated, $n = 27$ at 2 weeks, $n = 39$ at 4 weeks; and for *tl*/*tl* treated with CSF-1, $n = 27$ at both time points. Significance tests: $^{*}P < 0.00001$; $^{**}P < 0.01$; $^{***}P > 0.05$.

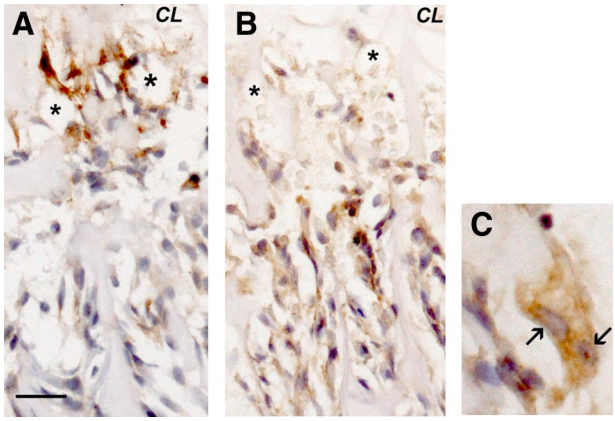

Figure 8. Septoclasts are negative for the CSF-1 receptor, c-Fms. Proximal tibial COJ of a 2-week-old normal littermate of the *tl* strain, labeled with anti-cathepsin B **(A)** or anti-c-Fms (**B** and **C**). Intensely labeled septoclasts are seen near capillaries (**asterisk**) in **A,** but no intense labeling with the anti-c-Fms antibody can be seen in the same region (**B**). A chondrocyte lacuna is labeled in **A** and **B** for orientation with respect to the growth plate. **C:** Osteoclast with two nuclei indicated by **arrows** is a positive control for c-Fms label and is enlarged from an area near that shown in **B.** Immunoperoxidase label with light hematoxylin counterstain. Scale bars: 25 μm (**A** and **B**); 12.5 μm (**C**).

Discussion

At the heart of endochondral ossification is the continuous invasion of cartilage by bone. The capillaries are on front line of the invasion and bring with them all of the cells of bone. The septoclast, extremely rich in the protease cathepsin B and associated with the advancing capillary front, is ideally positioned to provide an invasive path for budding vessels. *Csf1^{tl}/Csf1^{tl}* mutant rats develop severe postnatal growth plate dysplasia that becomes evident between the second and fourth weeks, when growth plates become markedly thicker, especially in the central region, chondrocyte hypertrophy fails to progress, and there is no evidence of vascular invasion.[14,23] We also knew from previous studies that CSF-1 injections restore metaphyseal osteoclasts and bone resorption but have no beneficial effect on the growth plate,[15,18] despite evidence of increased capillary budding at the COJ provided by CSF-1 injections.[14] Given the important role proposed for the septoclast in breaking down the terminal transverse cartilage septum of the growth plate and permitting vascular invasion, we hypothesized that this cell population would be deficient in *Csf1^{tl}/Csf1^{tl}* rats. We also wished to determine whether CSF-1 injections would restore septoclasts.

The septoclast counts in *Csf1^{tl}/Csf1^{tl}* correlate inversely with the growth plate dysplasia from age to age and region to region. At 2 weeks, at which age the dysplasia is less apparent, septoclasts are closer to normal in number and distribution. In addition, they are more normal in their appearance in those portions of mutant growth plates that show morphology closest to normal. For example, in the 4-week-old mutants, the central region of the growth plate is highly dysplastic. It becomes abnormally thick and there is no evidence of capillary invasion, whereas in the lateral regions, the dysplasia is less severe, and capillaries can be seen budding into the lower hypertrophic zone. The central region is virtually devoid of septoclasts. This relationship between the severity of the dysplasia and septoclast deficiency was observed consistently in the mutant animals.

We have shown previously that daily injections of CSF-1 in *Csf1^{tl}/Csf1^{tl}*rats do not resolve the growth plate dysplasia, even when treated from birth to up to 6 weeks, the longest time period that has been studied.[15] The growth plates remained dysplastic and nonmineralized, except for a layer of osteoid deposited directly onto the lower margin of the growth. This finding, together with the fact that 1 week of CSF-1 treatment restored septoclast counts to normal in 2-week-old mutants implies that, despite this normalization, the septoclasts were unable to direct capillary invasion and proper vascularization to the lower hypertrophic zone. By 4 weeks, although the counts did rebound somewhat in treated mutants, the response was far weaker. This result may reflect the greater starting difference between the mutant and wild-type animals at this age (Figure 7) or an age-dependant loss of responsiveness or cell plasticity. The fact that c-Fms was not detected in septoclasts (Figure 8) suggests that the effect of CSF-1 injections on septoclast populations is indirect.

In summary, septoclast counts correlated very well with the lack of vascular invasion of the growth in the mutant animals, but their restoration in CSF-1-treated animals did not bring about recovery of a normal endochondral process. Thus, there is an apparent contradiction in this model between septoclast numbers and their ability to perform their normal function. On the one hand, Aharinejad et al[14] showed increased angiogenesis at the distal femoral COJ of *Csf1^{tl}/Csf1^{tl}* animals treated for 3 weeks from birth. In that study the authors used vascular casts and scanning electron microscopy to enumerate capillaries and found greater capillary sprouting in CSF-1-treated mutants. On the other hand, we have shown previously that the growth plate chondrodysplasia of *Csf1^{tl}/Csf1^{tl}* rats treated from birth with CSF-1 does not improve even after 6 weeks of treatment, despite virtually complete, osteoclast-mediated removal of sclerotic bone from the metaphysis[15] and its replacement with hematopoietic marrow. Significantly, long bone growth was not restored in those treated mutants either. The growth plates remained dysplastic, consistent with a virtual lack of bone elongation at the time points studied. It therefore seems likely that in the study of Aharinejad et al,[14] the increased capillary sprouting reflected the vascularization of marrow and not of the growth plate itself, because the growth plate was not present in the macerated casts in which capillaries were counted, and so quantification of sprouting into the growth plate itself was not possible. To account for the inability of capillaries to invade the growth plate and to restore growth plate chondrocyte maturation and turnover, it seems likely that trophic factors arising in the growth plate chondrocytes themselves are needed to guide capillary ingrowth. This finding is consistent with an indirect effect of CSF-1 on septoclasts, especially considering their lack of c-Fms. Further, the mechanism responsible seems to be dependent, at least in part, on site-specific availability of CSF-1 and not sim-

ply on its systemic delivery via injection. If such a locally supplied signal is in fact required to direct capillary invasion and budding, and it weakens over time in this type of chondrodysplasia, it would explain why the septoclast is necessary but not sufficient to sustain vascular invasion at the COJ.

It is known that CSF-1 can induce VEGF expression in many normal tissues and in tumors. It is also known that the *tl* rat mutation is not the only osteopetrotic strain that develops progressive chondrodysplasia, with disorganized chondrocyte zones, thickening over time, and defective COJ vascularization. A careful examination of the literature shows that many osteopetrotic mutations, especially those that lack osteoclasts, have similar problems in endochondral progression.[13] Future studies may reveal the molecular mechanism for this gradual loss of cartilage turnover, bone elongation, and the directional recruitment of septoclasts and vasculature.

Acknowledgments

We extend our gratitude to Dr. John S. Mort of the Shiners' Hospital for Children, Montreal, QC, Canada, for making antibodies to rat cathepsins B and K available for this work. We thank Dr. Eunice Lee for discovering the septoclast and for much advice during these investigations. We thank our late colleague, Dr. Sandy C. Marks, Jr., for seminal contributions in the early phases of the project.

References

1. Marks SC Jr, Gartland A, Odgren PR: Skeletal development. Encyclopedia of Endocrine Diseases. Edited by Martini L. San Diego, Elsevier, 2004, pp. 261–272
2. Marks SC Jr, Odgren PR: The structure and development of the skeleton. Principles of Bone Biology. Edited by Bilezikian JP, Raisz LG, Rodan GA. New York, Academic Press, 2002, pp. 3–15
3. Davoli MA, Lamplugh L, Beauchemin A, Chan K, Mordier S, Mort JS, Murphy G, Docherty AJ, Leblond CP, Lee ER: Enzymes active in the areas undergoing cartilage resorption during the development of the secondary ossification center in the tibiae of rats aged 0–21 days: II. Two proteinases, gelatinase B and collagenase-3, are implicated in the lysis of collagen fibrils. Dev Dyn 2001, 222:71–88
4. Lee ER, Lamplugh L, Davoli MA, Beauchemin A, Chan K, Mort JS, Leblond CP: Enzymes active in the areas undergoing cartilage resorption during the development of the secondary ossification center in the tibiae of rats ages 0–21 days: I. Two groups of proteinases cleave the core protein of aggrecan. Dev Dyn 2001, 222:52–70
5. Kronenberg HM: Developmental regulation of the growth plate. Nature 2003, 423:332–336
6. Ballock RT, O'Keefe RJ: Physiology and pathophysiology of the growth plate. Birth Defects Res C Embryo Today 2003, 69:123–143
7. Breur GJ, VanEnkevort BA, Farnum CE, Wilsman NJ: Linear relationship between the volume of hypertrophic chondrocytes and the rate of longitudinal bone growth in growth plates. J Orthop Res 1991, 9:348–359
8. Farnum CE, Wilsman NJ: Determination of proliferative characteristics of growth plate chondrocytes by labeling with bromodeoxyuridine. Calcif Tissue Int 1993, 52:110–119
9. Wilsman NJ, Farnum CE, Green EM, Lieferman EM, Clayton MK: Cell cycle analysis of proliferative zone chondrocytes in growth plates elongating at different rates. J Orthop Res 1996, 14:562–572
10. Lee ER, Lamplugh L, Shepard NL, Mort JS: The septoclast, a cathepsin B-rich cell involved in the resorption of growth plate cartilage. J Histochem Cytochem 1995, 43:525–536
11. Van Wesenbeeck L, Odgren PR, MacKay CA, D'Angelo M, Safadi FF, Popoff SN, Van Hul W, Marks SC Jr: The osteopetrotic mutation toothless (tl) is a loss-of-function frameshift mutation in the rat Csf1 gene: evidence of a crucial role for CSF-1 in osteoclastogenesis and endochondral ossification, Proc Natl Acad Sci USA 2002, 99:14303–14308
12. Dobbins DE, Sood R, Hashiramoto A, Hansen CT, Wilder RL, Remmers EF: Mutation of macrophage colony stimulating factor (Csf1) causes osteopetrosis in the tl rat. Biochem Biophys Res Commun 2002, 294:1114–1120
13. Odgren PR, Philbrick WM, Gartland A: Perspective. Osteoclastogenesis and growth plate chondrocyte differentiation: emergence of convergence. Crit Rev Eukaryot Gene Expr 2003, 13:181–193
14. Aharinejad S, Marks SC Jr, Bock P, Mason-Savas A, MacKay CA, Larson EK, Jackson ME, Luftensteiner M, Wiesbauer E: CSF-1 treatment promotes angiogenesis in the metaphysis of osteopetrotic (toothless, tl) rats. Bone 1995, 16:315–324
15. Odgren PR, Popoff SN, Safadi FF, MacKay CA, Mason-Savas A, Seifert MF, Marks SC Jr: The toothless osteopetrotic rat has a normal vitamin D-binding protein-macrophage activating factor (DBP-MAF) cascade and chondrodysplasia resistant to treatments with colony stimulating factor-1 (CSF-1) and/or DBP-MAF. Bone 1999, 25:175–181
16. Seifert MF: Lack of evidence for rickets in the osteopetrotic rat mutation, toothless. J Bone Miner Res 1994, 9:1813–1821
17. Seifert MF: Abnormalities in bone cell function and endochondral ossification in the osteopetrotic toothless rat. Bone 1996, 19:329–338
18. Sundquist KT, Cecchini MG, Marks SC Jr: Colony-stimulating factor-1 injections improve but do not cure skeletal sclerosis in osteopetrotic (op) mice. Bone 1995, 16:39–46
19. Nakano K, Adachi Y, Minamino K, Iwasaki M, Shigematsu A, Kiriyama N, Suzuki Y, Koike Y, Mukaide H, Taniuchi S, Kobayashi Y, Kaneko K, Ikehara S: Mechanisms underlying acceleration of blood flow recovery in ischemic limbs by macrophage colony-stimulating factor. Stem Cells 2006, 24:1274–1279
20. Gerber HP, Vu TH, Ryan AM, Kowalski J, Werb Z, Ferrara N: VEGF couples hypertrophic cartilage remodeling, ossification and angiogenesis during endochondral bone formation. Nat Med 1999, 5:623–628
21. Yang M, Mailhot G, MacKay CA, Mason-Savas A, Aubin J, Odgren PR: Chemokine and chemokine receptor expression during colony stimulating factor-1-induced osteoclast differentiation in the toothless osteopetrotic rat: a key role for CCL9 (MIP-1γ) in osteoclastogenesis in vivo and in vitro. Blood 2006, 107:2262–2270
22. Hunziker EB, Herrmann W, Schenk RK: Improved cartilage fixation by ruthenium hexammine trichloride (RHT): a prerequisite for morphometry in growth cartilage. J Ultrastruct Res 1982, 81:1–12
23. Devraj K, Bonassar LJ, MacKay CA, Mason-Savas A, Gartland A, Odgren PR: A new histomorphometric method to assess growth plate chondrodysplasia and its application to the toothless (tl, $Csf1^{null}$) osteopetrotic rat. Connect Tissue Res 2004, 45:1–10